

Prediction of a Feshbach Resonance in the Below-the-Barrier Reactive Scattering of Vibrationally Excited HD with H

Boyi Zhou,^{†,‡} Benhui Yang,[†] N. Balakrishnan,[¶] B. K. Kendrick,[§] and P. C.
Stancil^{*,†}

[†]*Department of Physics and Astronomy and Center for Simulational Physics, University of Georgia, Athens, Georgia 30602, United States*

[‡]*Key Laboratory of Materials Modification by Laser, Electron, and Ion Beams (Ministry of Education), School of Physics, Dalian University of Technology, Dalian 116024, P. R. China*

[¶]*Department of Chemistry and Biochemistry, University of Nevada, Las Vegas, Nevada 89154, United States*

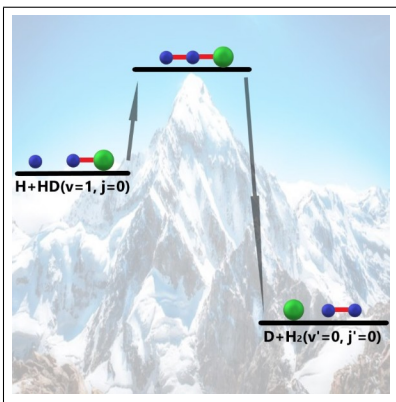
[§]*Theoretical Division (T-1, MS B221), Los Alamos National Laboratory, Los Alamos, New Mexico 87545, United States*

E-mail: pstancil@uga.edu

Abstract

Quantum reactive scattering calculations on the vibrational quenching of HD due to collisions with H were carried out employing an accurate potential energy surface. The state-to-state cross sections for the chemical reaction $\text{HD} (v = 1, j = 0) + \text{H} \rightarrow \text{D} + \text{H}_2 (v' = 0, j')$ at collision energies between 1 and 10,000 cm^{-1} are presented, and a Feshbach resonance in the low-energy regime, below the reaction barrier, is observed for the first time. The resonance is attributed to coupling with the vibrationally adiabatic potential correlating to the $v = 1, j = 1$ level of the HD molecule, and it is dominated by the contribution from a single partial wave. The properties of the resonance, such as its dynamic behavior, phase behavior, and lifetime, are discussed.

Graphical TOC Entry



The study of reactive collisions in atom-diatom systems is a very effective way to probe the interactions and reaction dynamics between atoms and molecules. Therefore, triatomic collision processes have played an important role in quantum dynamics, as they can give valuable insight into the chemical reaction mechanism.^{1,2} Because of their light mass and the availability of high-accuracy molecular potentials, H₂, HD, and D₂ are the most commonly studied molecular species and they serve as benchmark systems for state-to-state chemistry. Because of their high abundance in the interstellar medium, collisions of H₂ and HD with atomic hydrogen have attracted significant interest. For practical reasons, D + H₂³⁻⁶ and H + D₂⁷⁻¹¹ reactions have been studied rather extensively. HD, as the singly deuterated form of molecular hydrogen, is one of the products in these reactions. Because of the relatively large abundance of HD in space and its finite dipole moment, the observable properties of the collisional reaction of HD with H, such as cross sections and rate coefficients, are of particular interest.

Much attention has been devoted to the study of the H + HD reaction recently, stimulated by geometric phase effects in this system and the crucial role of HD in astrophysics.¹²⁻¹⁸ However, most of these studies, in particular those relevant to astrophysics, have investigated only rotational excitation of HD in its ground vibrational state. Vibrationally excited HD can be produced by a variety of processes in space, and thus, it is of interest to study its interaction with atomic hydrogen.¹⁹ Inspired by this point, we focus on the study of the reaction between vibrationally excited HD molecules and atomic hydrogen. The stereodynamics of rotational quenching of state-prepared HD in the $v = 1$ vibrational level in collisions with H₂, D₂, and He have also been reported recently.²⁰⁻²⁴ In this paper, we present results for the cross sections of the reactive processes for the H + HD collisional system when HD is in its first excited vibrational state ($v = 1$) and discuss the behavior of vibrational quenching of HD molecules due to collisions with H atoms. In particular, we report the presence of a narrow Feshbach resonance in the HD + H → D + H₂ reaction at energies below the reaction barrier that originates from coupling with the adiabatic potential correlating with

the $v = 1, j = 1$ level of the HD molecule.

A reliable potential energy surface (PES) for the H + HD system ensures the accuracy of the quantum dynamics calculations. Thus, an accurate description of the PES is required in order to obtain the cross sections for the reaction of H with HD. There are several PESs for the H₃ system that have been widely used in quantum-mechanical calculations. The best known are the LSTH,²⁵⁻²⁷ BKMP2,²⁸ and CCI²⁹ potentials. Among them, the BKMP2 and CCI potentials are considered the most accurate, and they reproduce most of the available experimental data. In our scattering calculations, we employed the CCI PES, but some comparisons are also provided on the BKMP2 PES. The CCI PES was developed with *ab initio* calculations of nearly full configuration interaction quality using a highly accurate many-body basis set extrapolation. There is a large barrier of about 3500 cm⁻¹ on this PES for the hydrogen exchange reaction with ground-state reactants, and the well depth of the global minimum is about 20 cm⁻¹.

In order to describe the reactive scattering of HD with H, the quantum-mechanical reactive scattering program ABC³⁰ was employed. To solve the Schrödinger equation, ABC uses a coupled-channel hyperspherical coordinate method for the motion of the three nuclei on a Born-Oppenheimer PES. The hyper-radius is divided into a large number of sectors, and in each sector the wave function is expanded in terms of ro-vibrational eigenfunctions of the diatomic fragments in each atom-diatom arrangement channel. For low collision energies, we used a large maximum hyper-radius and a large number of log derivative propagation sectors to ensure that the integration step size $\Delta\rho$ would be small enough to obtain converged results. With the convergence parameters used in ABC (see Table S1), the calculations were carried out for total angular momentum quantum numbers J from 0 to 120 in the range of collision energies from 1 to 10000 cm⁻¹. The results of the ABC program are the elements of the S-matrix in parity-adapted form. To obtain the collision energy variation of the cross sections for reactive processes, the elements of the S-matrix need to be converted from the parity-adapted form $S_{n'k',nk}^{J,P}(E)$ into standard helicity-representation form $S_{n'k',nk}^J(E)$.³⁰ Af-

ter the conversion, the reactive scattering integral cross sections (ICSs) can be calculated as

$$\sigma_{n'k' \leftarrow nk}(E) = \frac{\pi}{k_n^2} \sum_J (2J + 1) |S_{n'k',nk}^J(E)|^2, \quad (1)$$

where J is the total angular momentum quantum number, E is the collision energy, n and n' are composite indices for $\alpha v j$ and $\alpha' v' j'$ (in which α and α' are arrangement labels), k and k' are helicity quantum numbers, k_n is the wave vector (with $k_n^2 = \frac{2\mu E}{\hbar^2}$), and μ is the reduced mass of the system.

Figure 1 plots the state-to-state cross section as a function of collision energy for the reaction HD ($v = 1, j = 0$) + H \rightarrow D + H₂ ($v' = 0, j' = 0$). As can be seen, the cross section at low energies is small and decreases with increasing collision energy, reaching a global minimum at 84.69 cm⁻¹. The broader hump appearing at around 750 cm⁻¹ can be interpreted as metastable states of the H + HD reaction.³¹ The system passes through a transition state region along the reaction coordinate, and the maximum energy along the minimum-energy reaction pathway for the H + HD reaction is about 1036 cm⁻¹. Therefore, the cross section increases rapidly above a collision energy of 1000 cm⁻¹. Below this barrier, the reactivity can be attributed to quantum tunneling.

A striking feature of the results presented in Figure 1 is a sharp resonance peak that appears at 84.85 cm⁻¹, as shown in the inset. To our knowledge, this is the first time a resonance for the H₃ system has been predicted in this energy range and below the reaction barrier. In order to confirm this observation, we performed the calculation of state-to-state cross sections with different final states. Figure 2 presents the collision energy variation of cross sections for the HD ($v = 1, j = 0$) + H \rightarrow D + H₂ ($v' = 0, j'$) reaction with j' from 1 to 4. All of the resonance peaks are located at 84.85 cm⁻¹, but they vary in magnitude. The resonance peaks decrease in going from $j' = 1$ to 4, but it is worth noting that the peaks for $j' = 1$ and $j' = 2$ are larger than that for $j' = 0$. We also computed the total integral cross sections summed over all final states. As can be seen in Figure S1, the resonance survives in the total vibrationally resolved cross sections.

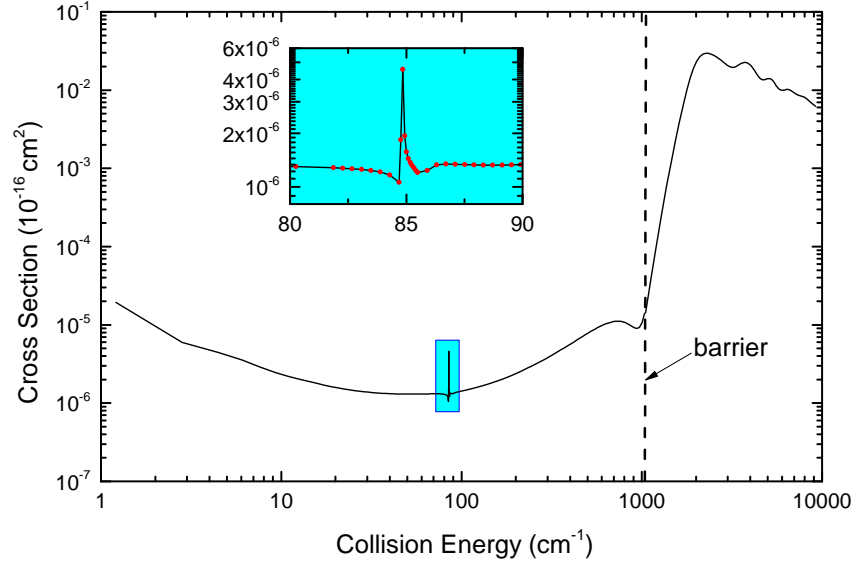


Figure 1: Collision energy variation of the cross section for the HD ($v = 1, j = 0$) + H \rightarrow D + H₂ ($v' = 0, j' = 0$) reaction. Inset: Feshbach resonance region.

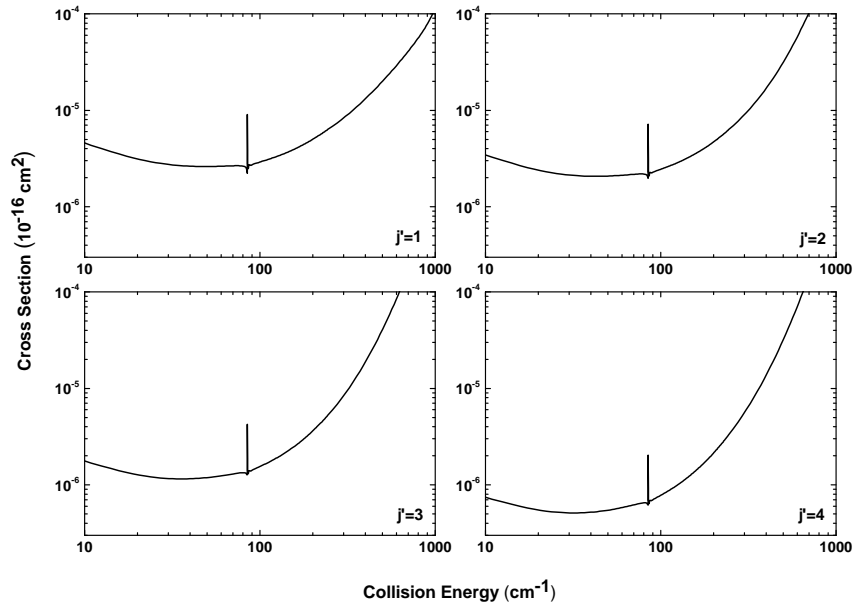


Figure 2: Collision energy variation of the cross sections for the HD ($v = 1, j = 0$) + H \rightarrow D + H₂ ($v' = 0, j'$) reaction with $j' = 1, 2, 3,$ and 4 .

Because resonance peaks are usually dominated by the contribution from a single partial waves or a narrow range of partial waves, the squares of the S -matrix elements $S_{n'k',nk}^J(E)$ for $J = 0 - 6$ are plotted in Figure 3 (we note that here the partial wave or orbital angular momentum L of H about HD is equal to J since $j = 0$). It is clear that $J = 1$ dominates the peak at 84.85 cm^{-1} . The behavior that $J = 1$ dominates the resonance can also be seen in the cross sections for j' from 1 to 3 (see Figure S2). As shown in Figure 3, the broader hump in the region of at about 750 cm^{-1} can be attributed to a nearly in-phase sum of J -resolved cross sections. To confirm that this resonance feature is not an artifact of the CCI PES or the ABC code used for the scattering calculations, separate quantum mechanical reactive scattering calculations were also carried out on the BKMP2 potential using the APH3D quantum mechanical reactive scattering program.^{32,33} Indeed, the BKMP2 PES also captures this resonance at exactly the same energy, though the magnitudes of the background cross sections from the two calculations differ at energies below the barrier where tunneling contributions become very sensitive to the details of the PESs and the basis sets employed in the ABC and APH codes (see Figure S3).

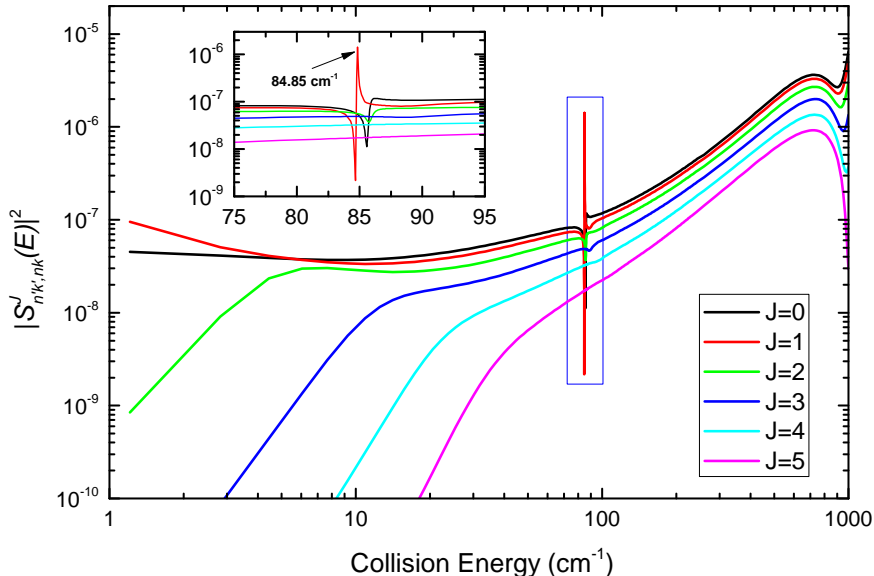


Figure 3: Collision energy variation of $|S_{n'k',nk}^J(E)|^2$ for the HD ($v = 1, j = 0$) + H \rightarrow D + H₂ ($v' = 0, j' = 0$) reaction for different values of the total angular momentum quantum number J .

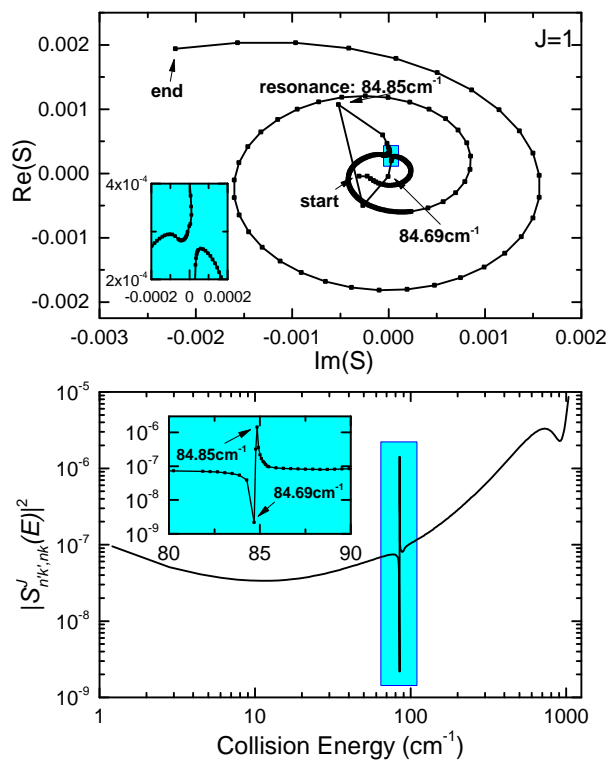


Figure 4: (top) Argand diagram for the HD ($v = 1, j = 0$) + H \rightarrow D + H₂ ($v' = 0, j' = 0$) reaction for $J = 1$. (bottom) Corresponding values of $|S_{n'k',nk}^J(E)|^2$.

To confirm that the resonance exhibits the proper phase behavior, an Argand diagram for the HD ($v = 1, j = 0$) + H \rightarrow D + H₂ ($v' = 0, j' = 0$) reaction for $J = 1$ is presented in Figure 4. The collision energy increases from 1.2 to 1033.6 cm⁻¹. The points were computed on a fine energy grid near the resonance to display its phase behavior. The background phase behavior corresponds to the smooth counterclockwise motion of the energy trajectory in the Argand plot. Near the resonance peak (blue inset), a kink in the Argand plot is observed where the resonance phase shift dominates and the trajectory temporarily reverses direction and exhibits a clockwise motion. The kink and associated clockwise loop in the Argand plot are a signature of a quantum resonance. Thus, the observation of the peak in the cross section is reconfirmed from the phase behavior. Specifically, the resonance point that we note in the Argand diagram corresponds to the sharp peak located at 84.85 cm⁻¹, and the contribution at 84.69 cm⁻¹ causes the global minimum of the cross section shown in Figure 1 at the same collision energy.

To gain more insight into the origin of the resonance, we examined the adiabatic potentials for the H + HD interaction for $J = 1$. Because the resonance occurs at about 85 cm⁻¹ relative to the $v = 1, j = 0$ level, it is most likely due to coupling with $v = 1, j = 1$ level of HD, which becomes energetically accessible at a collision energy of 85.37 cm⁻¹. Thus, it is very likely that this is a Feshbach resonance due to coupling with a quasi-bound state of the adiabatic potential correlating with the $v = 1, j = 1$ level of HD. For the initial $v = 1, j = 0$ state of HD only $L = 1$ contributes for $J = 1$. Thus, only odd inversion parity ($P = (-1)^{j+L} = -1$) contributes. For the $v = 1, j = 1$ level, odd-inversion-parity states for $J = 1$ that couple to the $v = 1, j = 0, L = 1$ channel are limited to $L = 0$ and 2. The corresponding adiabatic potentials are shown in Figure 5 as functions of the center-of-mass separation R between H and HD. The adiabatic potentials were computed by diagonalizing the interaction potential matrix at each value of R . Since the resonance occurs at the same energy for different j' levels of the product H₂, this is an entrance channel feature and we used reactant Jacobi coordinates and included only ro-vibrational levels of HD in constructing

the matrix elements of the interaction potential. It can be seen that the adiabatic potential corresponding to $v = 1$, $j = 1$, $L = 0$ supports a quasi-bound state at an energy of 84.82 cm^{-1} , which is very close to the energy of the resonance. The $v = 1$, $j = 1$, $L = 2$ potential does not support a bound state. We carried out similar analysis with the BKMP2 potential, which also supports a bound state for the $v = 1$, $j = 1$, $L = 0$ potential at 84.98 cm^{-1} (see Figure S4), consistent with a similar resonance feature at 85.33 cm^{-1} shown in Figure S3.

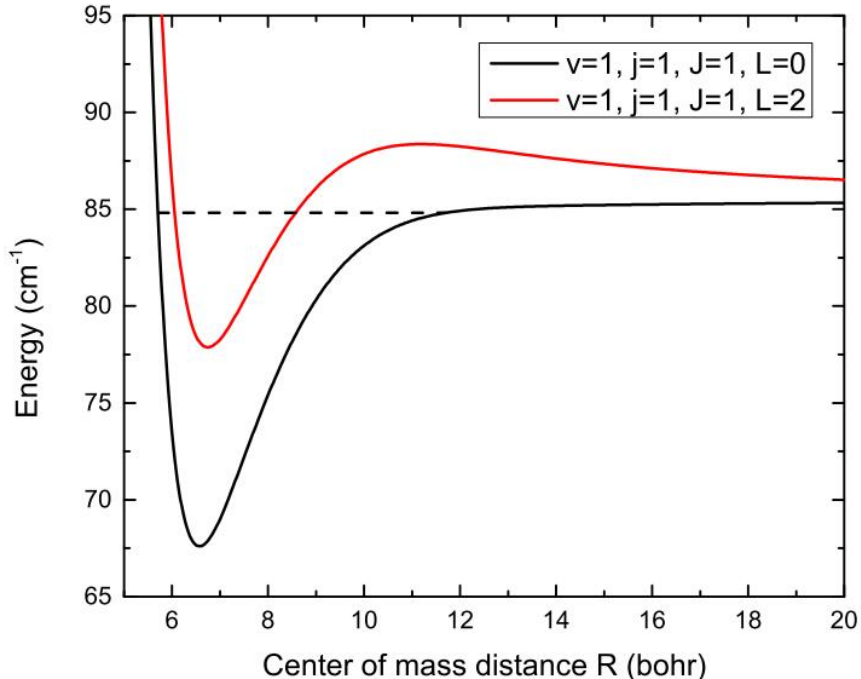


Figure 5: Adiabatic potentials correlating with different (v, j) states of HD in $\text{H} + \text{HD}$ ($v = 1$, $j = 0$) collisions for $J = 1$ on the CCI PES.

Resonances are often associated with metastable states of lifetime $\tau \simeq \hbar/\Gamma$, where Γ is the width of the resonance. To guide future experiments, we carried out a Lorentzian fit and extracted the lifetime. A very high resolution energy scan in the resonance region using Smith’s collision lifetime matrix formulation³⁴ was performed using the APH3D program on the CCI (BKMP2) PES. The results show that the lifetime is about 0.6 s (0.2 s) for this resonance state (see Figures S5 and S6). As can be seen, the lifetimes on the two PESs are very similar, and there is a slight shift in resonance energy: 85.37 cm^{-1} for CCI versus 85.33 cm^{-1} for BKMP2.

From an experimental point of view, a crossed-molecular-beam approach may be a good method to verify our theoretical prediction. A variety of experimental techniques have been developed over the past decade including, for example, Stark-induced adiabatic Raman passage (SARP),³⁵ the H-atom Rydberg tagging technique (HRTOF),^{36,37} the photoinitiated reaction method (PHOTOLOC),^{11,38,39} the velocity map ion imaging (VMI) technique,^{40,41} resonance-enhanced multiphoton ionization (REMPI) with UV pulses,⁴² and the quantum-state-specific backward scattering spectroscopy (QSSBSS) method.¹ SARP can be used to prepare HD molecules in a specific internal state. The HRTOF, PHOTOLOG, REMPI with UV pulses, and QSSBSS approaches can be used for detection. The Feshbach resonance is predicted to appear in a low-collision-energy region, be very narrow, and have a small magnitude. Therefore, an experimental approach will require very fine kinetic energy resolution and sensitivity.

In conclusion, quantum reactive scattering calculations for the H + HD ($v = 1, j = 0$) reaction were performed to obtain the collision energy variation of the cross section. A Feshbach resonance due to coupling with the $v = 1, j = 1, L = 0$ potential was found at about 85 cm^{-1} , which is significantly below the $\sim 1000 \text{ cm}^{-1}$ reaction barrier. In this reaction, the peak is dominated by the partial wave $L = 1$. The resonance is very longlived, with a lifetime close to a tenth of a second. We hope that these results stimulate experimental exploration of this resonance and further in-depth theoretical studies of this reaction.

Acknowledgement

Work at UGA was supported by NASA grant NNX16AF09G and at UNLV by NSF Grant No. PHY-1806334. The China Scholarship Council is acknowledged for supporting Boyi Zhou as a joint PhD student of the University of Georgia. B. K. Kendrick acknowledges that part of this work was done under the auspices of the U.S. Department of Energy under project No. 20170221ER of the Laboratory Directed Research and Development Program at Los

Alamos National Laboratory. Los Alamos National Laboratory is operated by Triad National Security, LLC, for the National Nuclear Security administration of the U.S. Department of Energy (Contract No. 89233218CNA000001). We thank Ionel Simbotin and Robin Côté for helpful discussions.

Supporting Information Available

The following files are available free of charge.

Parameters used in the calculations, cross sections summed over all final states, cross sections for different partial waves, comparisons of CCI-ABC and BKMP2-APH3D results, adiabatic potentials, and the lifetime of Feshbach resonance (PDF).

References

- (1) Yang, T.; Huang, L.; Xiao, C.; Chen, J.; Wang, T.; Dai, D.; Lique, F.; Alexander, M. H.; Sun, Z.; Zhang, D. H. *et al.* Enhanced reactivity of fluorine with para-hydrogen in cold interstellar clouds by resonance-induced quantum tunnelling. *Nat. Chem.* **2019**, *11*, 744–749.
- (2) Yang, T.; Yang, X. Quantum resonances near absolute zero. *Science* **2020**, *368*, 582–583.
- (3) Zhang, J. Z.; Miller, W. H. Quantum reactive scattering via the S-matrix version of the Kohn variational principle: Differential and integral cross sections for $D + H_2 \rightarrow HD + H$. *J. Chem. Phys.* **1989**, *91*, 1528–1547.
- (4) Takada, S.; Ohsaki, A.; Nakamura, H. Reaction dynamics of $D + H_2 \rightarrow DH + H$: Effects of potential energy surface topography and usefulness of the constant centrifugal potential approximation. *J. Chem. Phys.* **1992**, *96*, 339–348.

- (5) Aoiz, F. J.; Bañares, L.; Díez-Rojo, T.; Herrero, V. J.; Sáez Rábanos, V. Reaction cross section and rate constant calculations for the $D + H_2 (v = 0, 1) \rightarrow HD + H$ reaction on three *ab initio* potential energy surfaces. A quasiclassical trajectory study. *J. Phys. Chem.* **1996**, *100*, 4071–4083.
- (6) Bañares, L.; D’Mello, M. Quantum mechanical rate constants for the $D + H_2 \rightarrow HD + H$ reaction on the BKMP2 potential energy surface. *Chem. Phys. Lett.* **1997**, *277*, 465–472.
- (7) Yuan, D.; Chen, W.; Luo, C.; Tan, Y.; Li, S.; Huang, Y.; Sun, Z.; Yang, X.; Wang, X. Imaging the State-to-State Dynamics of the $H + D_2 \rightarrow HD + D$ Reaction at 1.42 eV. *J. Phys. Chem. Lett.* **2020**, *11*, 1222–1227.
- (8) Marinero, E. E.; Rettner, C. T.; Zare, R. N. $H + D_2$ reaction dynamics. Determination of the product state distributions at a collision energy of 1.3 eV. *J. Chem. Phys.* **1984**, *80*, 4142–4156.
- (9) Rinnen, K.-D.; Kliner, D. A.; Blake, R. S.; Zare, R. N. The $H + D_2$ reaction: “prompt” HD distributions at high collision energies. *Chem. Phys. Lett.* **1988**, *153*, 371–375.
- (10) D’Mello, M.; Manolopoulos, D. E.; Wyatt, R. E. Quantum dynamics of the $H + D_2 \rightarrow D + HD$ reaction: Comparison with experiment. *J. Chem. Phys.* **1991**, *94*, 5985–5993.
- (11) Gao, H.; Sneha, M.; Bouakline, F.; Althorpe, S. C.; Zare, R. N. Differential Cross Sections for the $H + D_2 \rightarrow HD (v' = 3, j' = 4 - 10) + D$ reaction above the Conical Intersection. *J. Phys. Chem. A* **2015**, *119*, 12036–12042.
- (12) Yuan, D.; Yu, S.; Chen, W.; Sang, J.; Luo, C.; Wang, T.; Xu, X.; Casavecchia, P.; Wang, X.; Sun, Z. *et al.* Direct observation of forward-scattering oscillations in the $H + HD \rightarrow H_2 + D$ reaction. *Nat. Chem.* **2018**, *10*, 653–658.

- (13) Yuan, D.; Guan, Y.; Chen, W.; Zhao, H.; Yu, S.; Luo, C.; Tan, Y.; Xie, T.; Wang, X.; Sun, Z. *et al.* Observation of the geometric phase effect in the $\text{H} + \text{HD} \rightarrow \text{H}_2 + \text{D}$ reaction. *Science* **2018**, *362*, 1289–1293.
- (14) Desrousseaux, B.; Coppola, C. M.; Kazandjian, M. V.; Lique, F. Rotational Excitation of HD by Hydrogen Revisited. *J. Phys. Chem. A* **2018**, *122*, 8390–8396.
- (15) Kendrick, B. K.; Hazra, J.; Balakrishnan, N. Geometric phase effects in the ultracold $\text{D} + \text{HD} \rightarrow \text{D} + \text{HD}$ and $\text{D} + \text{HD} \rightarrow \text{H} + \text{D}_2$ reactions. *New J. Phys* **2016**, *18*, 123020.
- (16) Kendrick, B. K.; Hazra, J.; Balakrishnan, N. Geometric phase effects in the ultracold $\text{H} + \text{H}_2$ reaction. *J. Chem. Phys.* **2016**, *145*, 164303.
- (17) Hazra, J.; Kendrick, B. K.; Balakrishnan, N. Geometric phase effects in ultracold hydrogen exchange reaction. *J. Phys. B: At., Mol. Opt. Phys.* **2016**, *49*, 194004.
- (18) Kendrick, B. K.; Hazra, J.; Balakrishnan, N. Geometric phase appears in the ultracold hydrogen exchange reaction. *Phys. Rev. Lett.* **2015**, *115*, 153201.
- (19) Kendrick, B. K. Nonadiabatic Ultracold Quantum Reactive Scattering of Hydrogen with Vibrationally Excited HD ($v = 5 - 9$). *J. Phys. Chem. A* **2019**, *123*, 9919–9933.
- (20) Perreault, W. E.; Mukherjee, N.; Zare, R. N. Quantum control of molecular collisions at 1 kelvin. *Science* **2017**, *358*, 356–359.
- (21) Perreault, W. E.; Mukherjee, N.; Zare, R. N. Cold quantum-controlled rotationally inelastic scattering of HD with H_2 and D_2 reveals collisional partner reorientation. *Nat. Chem.* **2018**, *10*, 561–567.
- (22) Croft, J. F.; Balakrishnan, N.; Huang, M.; Guo, H. Unraveling the Stereodynamics of Cold Controlled HD– H_2 Collisions. *Phys. Rev. Lett.* **2018**, *121*, 113401.
- (23) Croft, J. F.; Balakrishnan, N. Controlling rotational quenching rates in cold molecular collisions. *J. Chem. Phys.* **2019**, *150*, 164302.

- (24) Perreault, W. E.; Mukherjee, N.; Zare, R. N. HD ($v = 1, j = 2, m$) orientation controls HD–He rotationally inelastic scattering near 1 K. *J. Chem. Phys.* **2019**, *150*, 174301.
- (25) Liu, B. Ab initio potential energy surface for linear H₃. *J. Chem. Phys.* **1973**, *58*, 1925–1937.
- (26) Siegbahn, P.; Liu, B. An accurate three-dimensional potential energy surface for H₃. *J. Chem. Phys.* **1978**, *68*, 2457–2465.
- (27) Truhlar, D. G.; Horowitz, C. J. Functional representation of Liu and Siegbahns accurate abinitio potential energy calculations for H + H₂. *J. Chem. Phys.* **1978**, *68*, 2466–2476.
- (28) Boothroyd, A. I.; Keogh, W. J.; Martin, P. G.; Peterson, M. R. A refined H₃ potential energy surface. *J. Chem. Phys.* **1996**, *104*, 7139–7152.
- (29) Mielke, S. L.; Garrett, B. C.; Peterson, K. A. A hierarchical family of global analytic Born–Oppenheimer potential energy surfaces for the H + H₂ reaction ranging in quality from double-zeta to the complete basis set limit. *J. Chem. Phys.* **2002**, *116*, 4142–4161.
- (30) Skouteris, D.; Castillo, J.; Manolopoulos, D. ABC: a quantum reactive scattering program. *Comput. Phys. Commun.* **2000**, *133*, 128–135.
- (31) Der Chao, S.; Skodje, R. T. Signatures of reactive resonance: three case studies. *Theor. Chem. Acc.* **2002**, *108*, 273–285.
- (32) Kendrick, B.; Pack, R. T. Recombination resonances in thermal H + O₂ scattering. *Chem. Phys. Lett.* **1995**, *235*, 291–296.
- (33) Kendrick, B. K. Quantum reactive scattering calculations for the D + H₂ → HD + H reaction. *J. Chem. Phys.* **2003**, *118*, 10502–10522.
- (34) Smith, F. T. Lifetime matrix in collision theory. *Phys. Rev.* **1960**, *118*, 349–356.

- (35) Mukherjee, N.; Perreault, W. E.; Zare, R. N. *Frontiers and Advances in Molecular Spectroscopy*; Elsevier: Amsterdam, NL, 2018; pp 1–46.
- (36) Harich, S. A.; Dai, D.; Wang, C. C.; Yang, X.; Der Chao, S.; Skodje, R. T. Forward scattering due to slow-down of the intermediate in the $\text{H} + \text{HD} \rightarrow \text{D} + \text{H}_2$ reaction. *Nature* **2002**, *419*, 281–284.
- (37) Dai, D.; Wang, C. C.; Harich, S. A.; Wang, X.; Yang, X.; Der Chao, S.; Skodje, R. T. Interference of quantized transition-state pathways in the $\text{H} + \text{D}_2 \rightarrow \text{D} + \text{HD}$ chemical reaction. *Science* **2003**, *300*, 1730–1734.
- (38) Jankunas, J.; Zare, R. N.; Bouakline, F.; Althorpe, S. C.; Herráez-Aguilar, D.; Aoiz, F. J. Seemingly anomalous angular distributions in $\text{H} + \text{D}_2$ reactive scattering. *Science* **2012**, *336*, 1687–1690.
- (39) Jankunas, J.; Sneha, M.; Zare, R. N.; Bouakline, F.; Althorpe, S. C.; Herráez-Aguilar, D.; Aoiz, F. J. Is the simplest chemical reaction really so simple? *Proc. Natl. Acad. Sci. U. S. A.* **2014**, *111*, 15–20.
- (40) Eppink, A. T.; Parker, D. H. Velocity map imaging of ions and electrons using electrostatic lenses: Application in photoelectron and photofragment ion imaging of molecular oxygen. *Rev. Sci. Instrum.* **1997**, *68*, 3477–3484.
- (41) Lin, J. J.; Zhou, J.; Shiu, W.; Liu, K. Application of time-sliced ion velocity imaging to crossed molecular beam experiments. *Rev. Sci. Instrum.* **2003**, *74*, 2495–2500.
- (42) Zimmermann, R.; Mühlberger, F.; Fuhrer, K.; Gonin, M.; Welthagen, W. An ultracompact photo-ionization time-of-flight mass spectrometer with a novel vacuum ultraviolet light source for on-line detection of organic trace compounds and as a detector for gas chromatography. *J. Mater. Cycles Waste Manage.* **2008**, *10*, 24–31.